J Real-Time Image Proc (2009) 4:353–363
DOI 10.1007/s11554-009-0117-1

ORIGINAL RESEARCH PAPER

Sorting of rice grains using Zernike moments

Chong-Yaw Wee · Raveendran Paramesran · Fumiaki Takeda

Received: 7 January 2008 / Accepted: 24 February 2009 / Published online: 17 March 2009

Abstract Two important factors that determine the efficiency and reliability of a rice sorting machine are the overall processing speed and the classification accuracy. In this paper, an efficient rice sorting process which uses a subset of Zernike moments (ZM) and a multilayer perceptron is presented. Since the falling rice grains during sorting process can be in any orientation, a rotational invariant feature set is crucial in this application. Hence, the set of ZM with its inherent rotational invariance property is chosen in this context. Nevertheless, one of the main drawbacks of ZM in real-time application is its long computation time. To overcome this, a subset of ZM is selected from its original full set of 12 orders, using the combination of fuzzy ARTMAP and genetic algorithm. To further reduce the computation time, the combination of *q*-recursive method and Zernike polynomials' inherent symmetry property is utilized. Hence, the processing time of the subset of ZM is significantly reduced by almost 67% while maintaining the classification accuracy as compared to computing the original full set of ZMs.

C.-Y. Wee (✉) · R. Paramesran
Department of Electrical Engineering,
Faculty of Engineering, University of Malaya,
50603 Kuala Lumpur, Malaysia
e-mail: cywee2000@gmail.com

R. Paramesran
e-mail: ravee@um.edu.my

F. Takeda
Department of Intelligent Mechanical Systems Engineering,
Kochi University of Technology, Kochi, Japan
e-mail: takeda.fumiaki@kochi-tech.ac.jp

Keywords Rice sorting process · Zernike moments · Multilayer perceptron · Fuzzy ARTMAP · Genetic algorithms

1 Introduction

In the conventional rice sorting machine, the classification process is performed based on the color information criterion of the captured rice grain image frames. The examples of good (high quality) and damaged rice (low quality) grains in RGB color format are shown in Fig. 1. From Fig. 1, it is observed that the high-quality rice grains can be easily separated from the low-quality ones based on the shape and color criterion. High-quality rice grains normally have a smooth, clean and translucent white surface. In terms of shape, they normally show a short elliptical or elongated intact shape without any significant broken parts. Meanwhile, low-quality rice grains are normally either light or dark brown in color in parts or the whole surface of the grains. Sometimes, they may be milky white in color (not translucent) with rough or coarse in their surface. Besides that, the low-quality rice grains are normally shorter and not intact in shape with some broken parts if compared to high-quality rice grains. Similar conditions can be observed for foreign objects which exist in the unsorted rice grains such as dried grasses and seeds, broken glasses, small stones pieces, worms, broken ceramic and metal pieces, wood chips, etc. The examples of the foreign objects in unsorted rice grains are shown in Fig. 2. Most of them having significant distinct shape and color from the high-quality rice grains.

In the conventional rice-sorting process, the rice grain as it falls down from a shunt is captured and its color-tone values are compared with the predetermined threshold

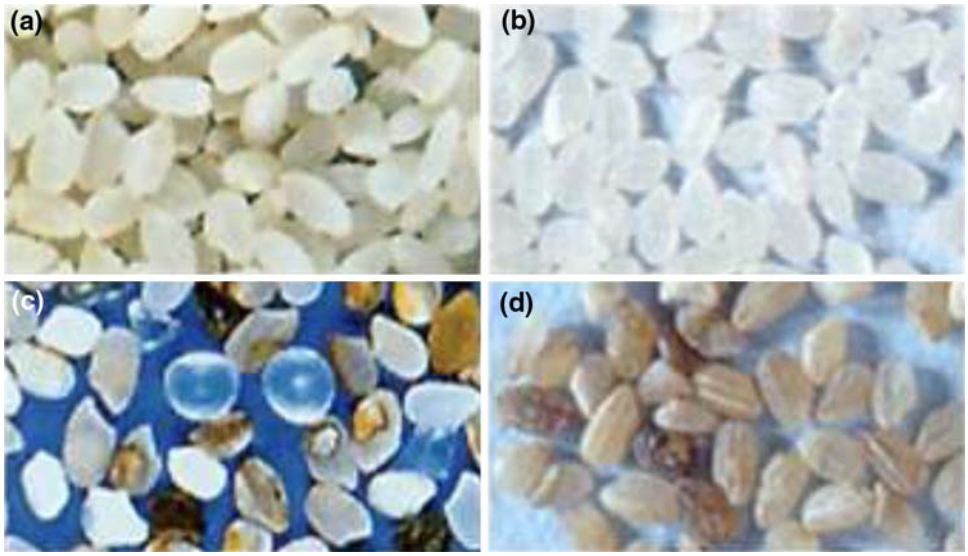

Fig. 1 Examples of high quality and low quality rice grains with **a** and **b** are high quality grains and **c** and **d** are low quality grains

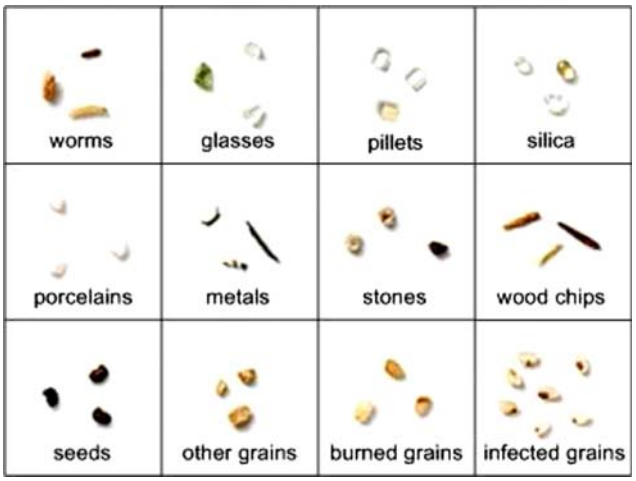

Fig. 2 Examples of foreign objects in the contaminated, unsorted rice grains

values. If the color-tone values are below the threshold values, then the rice grain or foreign object is considered as a low-quality grain, which will be rejected. However, in the classification of rice grain not only the color of the grain matters but also the shape. Therefore, in order to overcome this drawback, a more efficient pattern feature representation algorithm is required in the rice sorting system design.

Since the falling rice grain can be in any orientation and direction, a rotational invariant features set is crucial in this application. In this context, a set of orthogonal Zernike moments (ZM) with its inherent rotational invariance property [22, 26] makes it ideally suitable to be applied in proposed design. Other orthogonal basis functions such as Legendre moments, Krawtchouk moments and discrete cosine transform require special normalizations or transformations before achieving the rotational invariance property. Normally these normalizations or transformations are quite complex and sometimes do not provide exact invariant values.

The set of ZMs has been widely used in many applications in image analysis such as invariant patterns or object recognition [17, 29], image reconstruction [24], edge detection [10] and image segmentation [11]. ZMs have also been used in modeling the corneal surfaces [15]. The kernel of ZMs is a set of orthogonal Zernike polynomials which are defined in unit circle in polar format. With the orthogonal property, ZMs can be used to represent an image with minimum amount of information redundancy [20, 21, 25]. This property also enables one to separate out the individual contribution of each order moment (its information content) to the reconstruction process and hence eases the image reconstruction process from ZMs [18, 25]. The readers are referred to [16] to view the reconstruction power of each individual order of ZMs for English characters. The scaling and translation invariance properties of ZMs can be easily achieved through some normalizing processes in the computation of its polynomials [7, 8]. Additional to that, a set of ZMs is able to represent the statistical (mean and variance) and geometrical (centroid) information of an image concurently.

Besides the inherent rotational invariance property of ZMs, the morphological or shape characteristics of rice grain, which is ellipsoidal, is another crucial reason for the selection of ZMs in this project. The radial basic function of Zernike polynomials which can be represented in terms of sine and cosine functions is able to represent the shape of the object well. If the object is circular or ellipsoidal in nature, then a better representation of the shape of the object can be achieved. Lower order ZMs with low change rate of sine and cosine waveforms of Zernike polynomials are able to pick-up the information of the rice grains and provide a good representation. Hence a set of ZMs up to

12th order is sufficient to provide good representation of the shape of the rice grains. The shapes of low-quality rice grains and foreign objects such as worms, glass or porcelain pieces, stones and wood chips are very different from the ellipsoidal shape of the high-quality rice grains. Hence, the computed ZM values for these shapes are significantly different from those computed from the ellipsoidal shape of the high-quality rice.

Nevertheless, the main drawback of using the set of ZMs in real-time applications is its computational complexity which involves the computation of factorial terms. The computation of factorial terms is not only very time consuming but also leads to numerical instability especially for high order moments and/or large image size. Hence, many fast algorithms have been developed to bypass the computation of factorial terms. Chong et al. employ the recurrence relationships between successive Zernike polynomial coefficients to achieve the fast computation [5]. Another approach which uses the recurrence relationships between successive Zernike polynomials has also been proposed to increase the computation speed. Algorithms under this approach include Belkasim's [1], Prata's [23], Kintner's [19] and its simplified version (p-recursive) [28], and q-recursive [6] methods.

Recently, a fast computation method which is the combination of symmetry and q-recursive methods is proposed to reduce the computation time of ZMs [31]. The radial polynomials in Zernike polynomials are symmetry with respect to the principal x and y and diagonal axes. This implies that the computation of Zernike radial polynomials required is just within the first 45° instead of 360° in conventional method [31]. The application of this symmetrical property in q-recursive method has reduced the computation of ZMs by more than 50% [31]. This efficient approach makes the set of ZMs feasible to be used in real-time application.

The amount of time taken to process the image of each rice grain decides the separation distance of one grain from another (or the rice flow volume in sorting process). The closer the separation distance of one grain from another will lead to higher number of grains be imaged and processed in a given time (larger rice flow volume). Hence, the dimension of pattern features used to represent a rice grain image plays crucial role in determining the rice flow volume. ZMs up to 12 orders which contains 48 features has been used in several applications [16–18]. A faster processing time is accomplished if lesser number of ZMs is used. It is essential that using lesser ZMs does not compromise the classification performance. This motivates the authors to apply a subset of ZMs in feature extraction stage of the proposed design.

In this paper, a feature selection (dimension reduction) algorithm is proposed to reduce the number of ZMs used in the proposed rice sorting system. This algorithm is called evolutionary fuzzy ARTMAP (EFA) which uses genetic algorithms (GA) to determine the subset of ZM features and FA classifier to evaluate the classification performance of the selected subset [32]. GA is an optimization algorithm which is based on the mechanics of natural selection and natural genetics [9, 12–14, 27]. The performance of each population of a GA generation is evaluated using a fitness or objective function. This function is constructed based on the optimization criterion of applications which maximize the output performance. In the rice sorting application, two important criteria are included in constructing its fitness function, i.e., feature dimension and classification accuracy. Since one of the optimization criteria is the classification or sorting accuracy, a classifier is required to evaluate the selected GA population fitness or performance. This classifier must be relatively fast because GA incurs the cost of evaluating all the population of potential solutions. In this regard, FA classifier which learns and converges much faster (several iterations) than multilayer perceptron (MLP) classifier (thousands of iterations) [2–4] is applied to evaluate the GA population performance. Finally, this selected subset of ZMs is then used as the input pattern features to the MLP classifier to perform the sorting process. This classifier provides fast decision speed and good classification accuracy after proper training is provided [32].

The organization of this paper is given as follows. The proposed rice sorting process is briefly explained in Sect. 2. The basic concepts of ZMs are presented in Sect. 3. The fast computation of ZMs set using the fusion of q-recursive method and symmetry property of radial polynomials is explained in Sect. 4. The selection of the subset of ZMs using GA and FA classifier is presented in Sect. 5. The performance of the proposed design is presented in Sect. 6. Section 7 concludes the study.

2 Proposed rice sorting process

The novel rice sorting process proposed in this paper is based on the ZM feature extractor and neural network classifier. The main purpose of the proposed process is to improve the reliability and efficiency of conventional rice sorting machines. Figure 3 shows the hardware architecture of the proposed rice sorting machine design. Figure 4 shows the prototype that is used in the classification of rice grain using the proposed process.

The sorting machine consists of a magnetic feeder to direct all the rice grains to a shunt where the falling rice grain is captured by the color sensor. The captured image is in 24-bit RGB bitmap format (256-color). In order to reduce the noise effects during imaging process and to

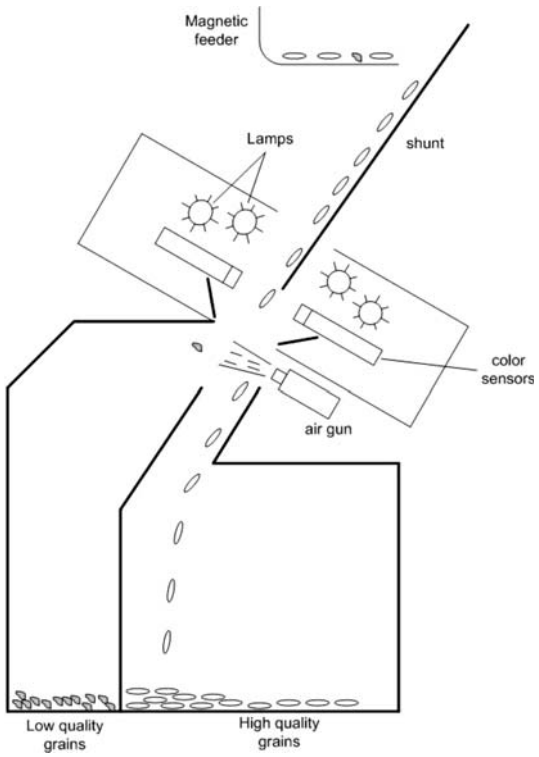

Fig. 3 Hardware architecture of the proposed rice sorting machine

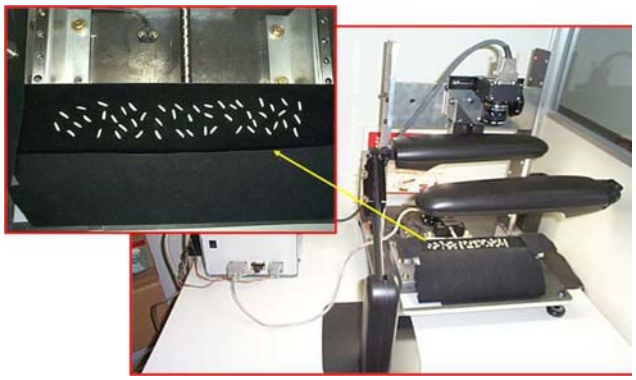

Fig. 4 Prototype of the proposed rice sorting system

reduce the computational complexity, only the blue color data is extracted from RGB color information. The blue color data produces better results in this application by minimizing the noise effects caused by the shadows from other rice grains. The image is then converted into binary format using a predefined threshold value on the blue-color component. The binarized image contains pixel values in terms of '0' and '1', with '1' denotes rice and '0' denotes background.

Since the captured image contains several cascaded rice grains, a segmentation algorithm is required to separate them into single disjointed grain image. A simple eight-nearest-neighbor connectivity criterion is applied in the

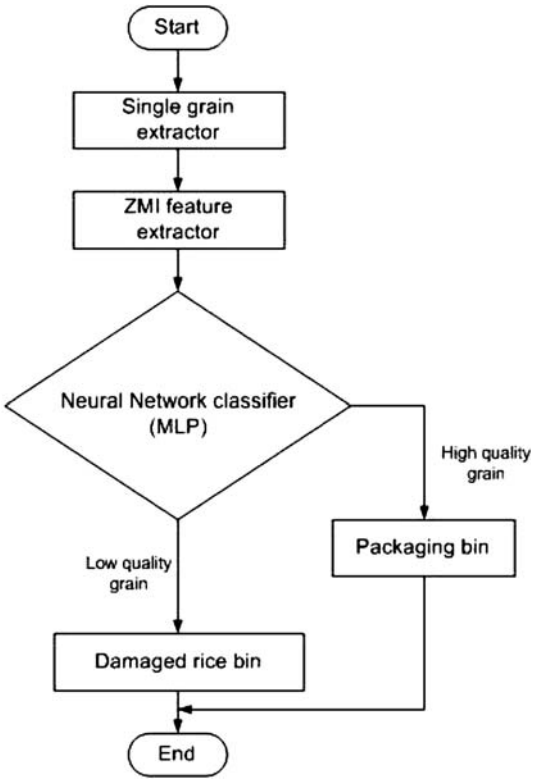

Fig. 5 Sorting transaction flow chart

separation process. In this operator, a pixel of '1' is searched and a current labeled number is given when the pixel of value '1' is found. If the pixel of '1' is at the eight neighbors of the current labeled number, the pixel is numbered to the current labeled number. If the pixel of '1' is not at the eight neighbors of the current labeled number, a new labeled number is given to that pixel. This segmentation process is repeated until all disjointed rice grains are obtained. Individual labeled number of every rice grain is used later as the indicator for the air guns to separate the different qualities of rice grains.

Then a ZMs-based feature extractor is used to extract features from the binarized individual rice grain image. The computed ZM features are then fed into a well-trained MLP classifier to determine the quality of the rice grain. If the rice grain belongs to a low quality then the air gun is activated which directs the low-quality rice grains into a bin reserved for low-quality rice grains.

The flow chart of the sorting transaction of the proposed rice sorting process is shown in Fig. 5.

3 Zernike moments

Zernike functions introduced by Frits Zernike, a Dutch mathematician and physicist, is a set of complex functions

with a simple rotational invariance property and forms a complete orthogonal basis over the class of square integrable functions defined over the unit circle [33]. The kernel of ZMs is a set of orthogonal Zernike polynomials defined over polar coordinates inside a unit circle.

The p-order Zernike polynomial with repetition q, $V_{pq}(r,\theta)$ is defined in polar coordinate system as [33]

$$V_{pq}(r,\theta) = R_{pq}(r)e^{jq\theta} \tag{1}$$

where $r = \sqrt{x^2+y^2}$, $\theta = \arctan(y/x)$ is the angle between the vector r and the principal x-axis. The real-valued Zernike radial polynomial, $R_{pq}(r)$ is given as

$$R_{pq}(r) = \sum_{k=q}^{p} B_{pqk} r^k \tag{2}$$

where $p - |q|$ is even, $0 \le |q| \le p$ and coefficients B_{pqk} are computed as

$$B_{pqk} = \frac{(-1)^{\frac{p-k}{2}}\left(\frac{p+k}{2}\right)!}{\left(\frac{p-k}{2}\right)!\left(\frac{k+q}{2}\right)!\left(\frac{k-q}{2}\right)!} \tag{3}$$

The Zernike polynomials can be rewritten in terms of real-valued radial polynomials, $S_{pq}(r)$ as

$$V_{pq}(r,\theta) = \sum_{k=q}^{p} B_{pqk} r^k e^{jq\theta} = \sum_{k=q}^{p} B_{pqk} S_{pq}(r) e^{jq\theta} \tag{4}$$

The set of Zernike polynomials, $V_{pq}(r,\ \theta)$ forms a complete orthogonal set on the interval $[-1,\ 1]$:

$$\int_{-\pi}^{\pi}\int_{-1}^{1} V_{pq}(r,\theta)[V_{p'q'}(r,\theta)]^* r\,dr\,d\theta = \begin{cases} \frac{\pi}{p+1}\delta pp'\delta qq' & p = p', q = q' \\ 0 & \text{otherwise} \end{cases}. \tag{5}$$

and its real-valued radial polynomials also satisfy the orthogonality relation as

$$\int_{-1}^{1} R_{pq}(r)[R_{p'q}(r)]^* r\,dr = \begin{cases} \frac{1}{2(p+1)}\delta_{pp'} & p = p', \\ 0 & \text{otherwise} \end{cases}. \tag{6}$$

where δ_{ij} is the Kronecker delta.

The two-dimensional ZM of order p with repetition q of an image intensity function $f(x,y)$ is defined as

$$Z_{pq} = \frac{p+1}{\pi}\int_{-\pi}^{\pi}\int_{-1}^{1}\sum_{k=q}^{p} B_{pqk} r^k e^{-jq\theta} f(r,\theta) r\,dr\,d\theta \tag{7}$$

with $dx\ dy = r dr\ d\theta$ and $-\pi \le \theta \le \pi$.

The set of ZMs possesses the inherent rotational invariance property. The invariant features are obtained by taking the magnitude values of ZMs since they remain the same to those image functions before and after rotation. The rotation invariant ZM is extracted by considering only their magnitude values as

$$|Z^r_{pq}| = |Z_{pq}e^{-jq\alpha}| = |Z_{pq}| \tag{8}$$

where Z^r_{pq} is the ZM computed from the rotated image. Only the magnitude of ZMs with $q \ge 0$ is used since $Z_{p,-q} = Z^*_{pq}$ and $|Z_{p,q}| = |Z_{p,-q}|$ [16, 18]. The scaling and translation invariance properties of ZMs can be easily achieved through some normalization processes [7, 8].

4 Fast computation of Zernike moments

The fast computation algorithm of ZMs used in the proposed design is a combination of the q-recursive method and symmetrical property of radial polynomials. Basic properties which contribute to the fast computation of these methods are presented in this section.

4.1 q-recursive method

The recurrence relation in terms of repetition q between the Zernike radial polynomials of same order is given as [6]

$$R_{pq}(r) = H_1 R_{p(q+4)}(r) + \left(H_2 + \frac{H_3}{r^2}\right) R_{p(q+2)}(r) \tag{9}$$

where the recurrence coefficients, H_1, H_2 and H_3 are defined as

$$\begin{aligned} H_1 &= \frac{q(q-1)}{2} - qH_2 + \frac{H_3(p+q+2)(p-q)}{8} \\ H_2 &= \frac{H_3(p+q)(p-q+2)}{4(q-1)} + (q-2) \\ H_3 &= -\frac{4(q-2)(q-3)}{(p+q-2)(p-q+4)} \end{aligned} \tag{10}$$

This method is only applicable for cases $(p - q \ge 4)$ as shown in (9). For cases $(p - q \le 2)$, $R_{pq}(r)$ are computed using following relation

$$\begin{aligned} &R_{pp}(r) = r^p \quad \text{for } (p = q) \\ &R_{p(p-2)}(r) = pR_{pp}(r) - (p-1)R_{(p-2)(p-2)}(r) \quad \text{for } (p - q = 2) \end{aligned} \tag{11}$$

This is a cross-repetition method and is not suitable for the computation of ZMs which are from different orders of p where the computation of the full set of $R_{pq}(r)$ are required.

4.2 Symmetry property of radial polynomials

In ZMs computations, a $(N \times N)$ square image is mapped into the unit circle of radial polynomials as shown in Fig. 6.

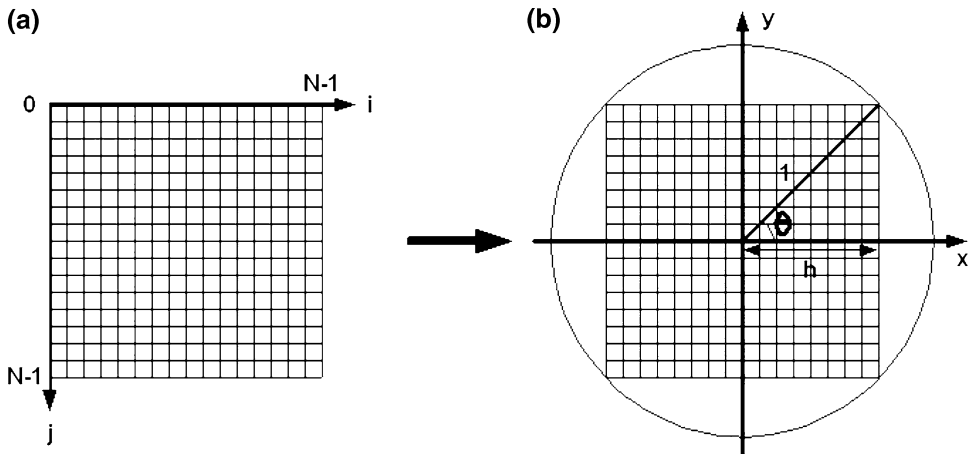

Fig. 6 **a** ($N \times N$) square image. **b** Mapping of square image into unit circle of radial polynomials (Figure excerpted from [31, 32])

The general formula of this mapping technique is given as

$$x_i = c_1 i + c_2; \quad y_j = c_1 j + c_2 \tag{12}$$

where the coefficients c_1 and c_2 are given as

$$c_1 = \frac{2h}{N-1}; \quad c_2 = -h \tag{13}$$

with $0 \leq h \leq 1$ and $h \in R$.

Zernike polynomials, $V_{pq}(r, \theta)$ can be separated into two parts, i.e., the real-valued radial polynomials, r^p and the exponential angle term, $\exp(jq\theta)$ [31]. With this mapping, the r values are symmetry at the principal x-, y- and $x = y$ axes. The minimum value of r that at the image edge in Fig. 6 is given as $r = h = 1/\sqrt{2}$. It will achieve its maximum value, i.e., $r = 1$ at $\theta = 45°$. As the θ value increases again, the r value starts to decrease from its maximum value back to $1/\sqrt{2}$ at $\theta = 90°$. The increment and decrement trends of r value are similar for all other inner pixels. Furthermore, the increment of r value for $0° \leq \theta \leq 45°$ is the same with the decrement of r value for $45° \leq \theta \leq 90°$. Hence, within a quadrant, only about half of the r values are needed to be computed. Similar conditions are observed in the remaining three quadrants because the r value of each pixel is repeating for every 45°. Therefore, the computation of r can be reduced to just within the first 45° and is able to achieve about 87.5% of the computation of entire set [31].

Let θ be the angle between the radius vector, r and the principal x-axis as shown in Fig. 6, then θ value is computed as

$$\theta = \tan^{-1}\left(\frac{y}{x}\right) \tag{14}$$

The θ values in the first and fourth quadrants of a square image are both the same except for their signs. All the θ values in first quadrant are negative while they are positive in the fourth quadrant. Similarly, the second and third quadrants also exhibit the same characteristics as the first and fourth quadrants where all the θ values are negative and positive in the second and third quadrants, respectively. These θ values are symmetry to the principal x-axis and hence their computation can be reduced to just the first 180° with 50.0% of reduction [31].

4.3 Fast computation using the fusion of q-recursive method and symmetry property

Since the captured rice grain image is in discrete Cartesian coordinate format, the computation of ZMs using (7) is approximated in discrete format as [18, 26]

$$Z_{pq} = \lambda_p \sum_{x=0}^{N-1} \sum_{y=0}^{N-1} f(x,y) \mathrm{e}^{-jq\theta} \times [R_{pq}(x,y)] \tag{15}$$

where $R_{pq}(x, y) = R_{pq}(r)$ is the real-valued Zernike radial polynomials at image pixel (x, y) with $r = \sqrt{x^2 + y^2}$. The computation of factorial terms in (3) is simplified using the q-recursive method as shown in previous subsection.

The computation of ZMs using the q-recursive method is further simplified with the integration of the symmetrical property. It is performed by first computing the ZMs in the first quadrant of a ($N \times N$) square image as [31]

$$Z_{pq} = \lambda_p \sum_{x=0}^{\frac{N-1}{2}} \sum_{y=0}^{x} f(x,y) \mathrm{e}^{-jq\theta} \times \left[R_{pq}(x,y) + R_{pq}\left(\frac{N-1}{2} - x, \frac{N-1}{2} - y \right) \right] \tag{16}$$

After obtaining the moment values of the first quadrant, the entire set of radial moment functions can be obtained as [31]

$$Z_{pq} = \lambda_p \sum_{x=0}^{N-1}\sum_{y=0}^{N-1} f(x,y)\mathrm{e}^{-jq\theta} \times \left[R_{pq}(x,y) \quad \text{for } 0 \le x,y \le \frac{N-1}{2} \right.$$
$$+R_{pq}(N-1-x,y) \quad \text{for } \frac{N-1}{2} \le x \le N-1, 0 \le y \le \frac{N-1}{2}$$
$$+R_{pq}(x,N-1-y) \quad \text{for } 0 \le x \le \frac{N-1}{2}, \frac{N-1}{2} \le y \le N-1$$
$$\left. +R_{pq}(N-1-x,N-1-y) \quad \text{for } \frac{N-1}{2} \le x,y \le N-1 \right] \tag{17}$$

By applying (17) the computation time of ZMs is reduced significantly by around 50.0% [31].

5 Evolutionary fuzzy ARTMAP (EFA)

An optimization algorithm which is named as EFA is used in selecting a subset of ZMs from its full set. EFA uses the characteristics of GAs and FA classifier in performing the optimization process. The main objective of applying EFA is to identify a subset from a full set of 12 orders ZMs to improve the computational efficiency of the proposed process while maintaining its classification accuracy. Only up to 12 orders of ZMs are used in the proposed design because they provide a good and sufficient representation of image information for segmented simple binary shape as shown in [16, 18]. In this context, the optimization criteria used in the EFA are minimum number of ZMs used and without compromising the classification accuracy as given in (18). The advantages of using a subset of ZMs are: (1) reduction in the computation time required to compute ZMs and (2) simplification in the classification process with lesser inputs (subset of ZMs) to the neural network classifier.

The flow chart of EFA used in this application is shown in Fig. 7, while the procedure of the proposed EFA is provided in Table 1.

Every generation in EFA contains 25 binary strings and in each string the bits are randomly generated. Since ZMs up to 12 orders are used in this study, we need to use 48 bits to represent each one of them (not including the Z_{00}). A value of '1' denotes that the corresponding ZM is selected, while a value of '0' denotes that ZM is not selected.

The full set of 12 orders of ZMs computed from the rice images is used in training. Only the ZMs where their corresponding bits in binary strings is '1' are selected to perform the training and validation processes. After the training is completed, another set of rice images which also has the same selected ZM features is used in the validation. The classification accuracy of each string is used in determining the fitness function of GA.

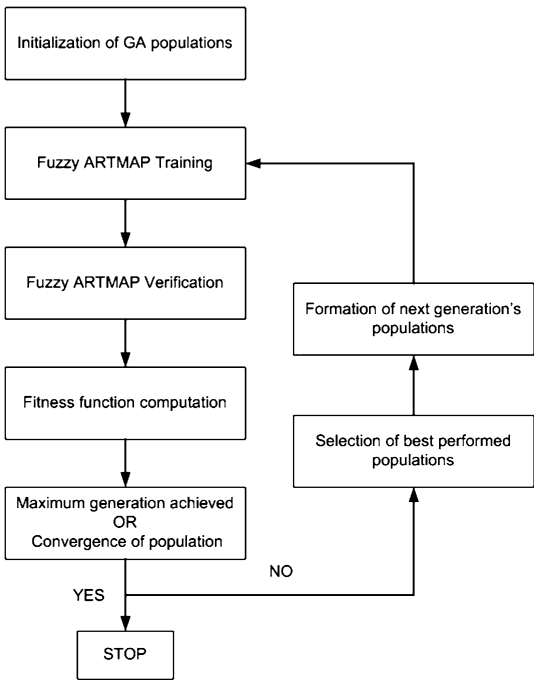

Fig. 7 Flow chart of the EFA algorithm for selecting the reduced-dimension subset Zernike moment features

The fitness function is a function that quantifies the optimality of a solution (that is, a chromosome) in GA so that particular chromosomes may be ranked against all the other chromosomes. The fitness function used in this application consists of the sum of two ratios as given in (18). The first ratio is the percentage of patterns classified correctly (classification accuracy), while the second ratio is the percentage of the ZMs which are not selected (number of features used). This GA fitness function serves to maximize the classification performance while equally minimizing the number of selected ZMs. This procedure is repeated for every string in the generation.

After obtaining the fitness score of all strings in one generation, the next generation (offsprings) is created using these fitness scores and the principle of GA—*survival of the fittest*. Tournament selection is applied during reproduction where the strings of next generation are reproduced from a small pool of strings chosen randomly from the strings in current generation. Among the strings in the small poll, only the best string (highest fitness score) is selected to be reproduced in next generation.

A single point crossover is used with a reasonable probability to exchange the information between strings, which introduces new characteristics to the next generation. Most of the mutations will destroy the 'good' characteristics carried by strings. Therefore, the probability of mutation is set relatively low to prevent too much mutation when the strings nearly approach convergence. In this study, the crossover and mutation probabilities are set to 0.25 and 0.04,

Table 1 Algorithms of evolutionary fuzzy ARTMAP (EFA)

Step 1:Initialization of GA populations

Each string of a generation consists of 48 binary bits.

Each string is randomly generated and is different from the others.

There are 25 strings in each generation to prevent the convergence problem.

Each bit represents a particular Zernike moment.

Bit '0' denotes the not-selection of Zernike moment while bit '1' denotes the selection of Zernike moment.

Step 2:Calculation of fitness function

The '1's in the string identifies the Zernike moment that is used for training and validation using fuzzy ARTMAP (FA) classifier.

The fitness function of each string is determined using the FA classification accuracy and the percentage of not selected features

$$\text{fitness}_{\text{string}} = \frac{\text{Pattern}_{\text{correct}}}{\text{Pattern}_{\text{total}}} + \frac{\text{features}_{\text{not-selected}}}{\text{features}_{\text{total}}} \quad (18)$$

where $\text{Pattern}_{\text{correct}}$ represents FA correctly classified patterns, $\text{Pattern}_{\text{total}}$ represents total patterns in the validation data, $\text{features}_{\text{not-selected}}$ represents number of not-selected features and $\text{features}_{\text{total}}$ represents total number of features.

Step 3: Generation of GAs populations for next generation

GA populations for next generation are generated using three GA operators namely reproduction, crossover and mutation based on the population fitness function calculated in Step 2.

Tournament selection is applied to randomly select the reproduction populations from a small pool of strings.

Single point crossover is applied to introduce new populations into next generation which will increase the convergence speed.

Mutation with small rate is applied to introduce new characteristics in next generation.

The number of strings in new generation is maintain same with the previous generation.

Step 4: Iteration

GA strings in new generation will undergo Steps 2–3 until convergence is achieved or when it reaches the predefined limitations.

respectively. The GA optimization process will repeat for maximum of 500 generations or if the fitness functions are larger than a predefined threshold value. The optimizing process will also stop if 20 out of 25 strings of a generation are same. After the optimization process, the selected ZMs are considered as the optimal features and are used as the input features for the neural network classifier.

Although the combination of GA with other neural network architectures such as MLP trained using back-propagation learning algorithm can be applied, but the slow convergence speed of MLP type neural networks during the learning process and along with multiple generation execution by GA make this process very expensive in terms of computation time [30]. Therefore, FA as a relatively faster classifier is used in order to reduce the complexity of optimization process of EFA. Besides the advantage in terms of convergence time, the FA classifier performs stable, on-line, incremental learning where it can learn from new inputs without retraining the earlier training data set [3, 4].

The subset of ZMs selected after optimization process using EFA is shown in Table 2.

6 Experimental study

Experiments are performed in order to verify the feasibility and efficiency of the proposed design for rice sorting system. The block diagram of the detail data flow in the experiment process is given in Fig. 8.

6.1 Experimental setup

The experiment begins by capturing the image of the falling rice grain using a color image sensor. The captured image normally contains several rice grains and is in 24-bit RGB color format. Hence, a segmentation algorithm is applied to separate them to obtain their individual rice grain image. The blue color information of the individual rice grain image is extracted and ZMs set is computed using this information. The computed ZMs set is then fed into a well-trained MLP classifier to determine the quality of the tested rice grain. The performance of the rice sorting machine is verified based on the classification accuracy of all tested rice grains.

The MLP classifier used is a three-layer network with single hidden layer and is trained using backpropagaiton learning algorithm. The input layer receives input from pattern features while the output layer contains two output nodes to represent two classes of rice grains, i.e., the high- and low-quality rice grains. In the training process, 50 individual rice grain images which are randomly chosen from the data set are used. The training process is conducted until the average error falls below 0.0001 or reaches a maximum epoch limit of 10,000.

6.2 Classification performance

A comparison of the full set of 12 orders and the selected subset of ZMs is performed in order to verify their

Table 2 The selected subset Zernike moment features determined by EFA

Zernike moments (Z_{pq})	Selected ($\surd$)/ not-selected ($\times$)	Zernike moments (Z_{pq})	Selected ($\surd$)/Not-selected ($\times$)
$Z_{1,1}$	$\surd$	$Z_{9,1}$	$\times$
$Z_{2,0}$	$\times$	$Z_{9,3}$	$\surd$
$Z_{2,2}$	$\times$	$Z_{9,5}$	$\times$
$Z_{3,1}$	$\surd$	$Z_{9,7}$	$\surd$
$Z_{3,3}$	$\surd$	$Z_{9,9}$	$\times$
$Z_{4,0}$	$\times$	$Z_{10,0}$	$\surd$
$Z_{4,2}$	$\surd$	$Z_{10,2}$	$\times$
$Z_{4,4}$	$\surd$	$Z_{10,4}$	$\surd$
$Z_{5,1}$	$\times$	$Z_{10,6}$	$\times$
$Z_{5,3}$	$\times$	$Z_{10,8}$	$\times$
$Z_{5,5}$	$\times$	$Z_{10,10}$	$\times$
$Z_{6,0}$	$\times$	$Z_{11,1}$	$\times$
$Z_{6,2}$	$\times$	$Z_{11,3}$	$\times$
$Z_{6,4}$	$\times$	$Z_{11,5}$	$\times$
$Z_{6,6}$	$\times$	$Z_{11,7}$	$\times$
$Z_{7,1}$	$\times$	$Z_{11,9}$	$\times$
$Z_{7,3}$	$\times$	$Z_{11,11}$	$\times$
$Z_{7,5}$	$\surd$	$Z_{12,0}$	$\times$
$Z_{7,7}$	$\surd$	$Z_{12,2}$	$\times$
$Z_{8,0}$	$\times$	$Z_{12,4}$	$\surd$
$Z_{8,2}$	$\surd$	$Z_{12,6}$	$\surd$
$Z_{8,4}$	$\times$	$Z_{12,8}$	$\surd$
$Z_{8,6}$	$\surd$	$Z_{12,10}$	$\times$
$Z_{8,8}$	$\surd$	$Z_{12,12}$	$\times$

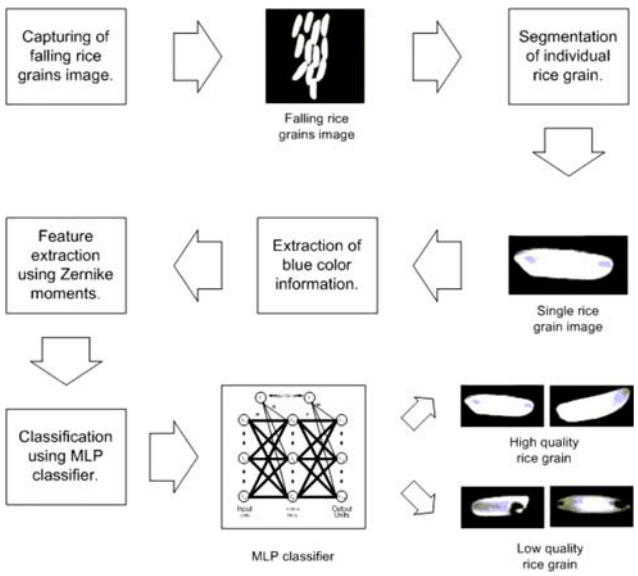

Fig. 8 Block diagram of the classification of rice grain

performances in terms of computation efficiency and classification accuracy. Two MLP classifiers of similar structure are trained using the backpropagation learning algorithm of same parameters and experimental conditions except for the number of input features fed into the input layer of MLP classifier. The first MLP classifier possesses 48 inputs which comprises the full 12 orders ZMs, while the second MLP classifier is trained using the subset, which contains 17 ZMs as shown in Table 2. The training and verification processes for both types of inputs are repeated by varying the number of hidden neuron from 5 to 30 in steps of 5.

The classification performances of the MLP classifier using the full set and the subset of ZMs are shown in Table 3. The results showed that the classification percentage using the full set ZMs varies with the variation in the number of hidden nodes while it is constant for the case of the subset of ZMs. The average accuracy of MLP classifier using the full set and the subset of ZMs are 95.0 and 98.0%, respectively. The percentage of computational time saved using the subset of ZMs when compared to the full set is provided in Table 3. Using the selected subset of ZMs, the proposed design reduces the average overall processing time by 67.55%.

Since the classification accuracy and significant reduction in processing time are achieved, the selected subset of ZMs can be applied in real-time rice sorting machine. Once the subset of ZMs is selected, it can be used throughout the rice sorting process. Each time when a new process begins, the system first needs to be recalibrated with good and rejected rice grains. This will eliminate any changes in the settings such as illumination. Hence, the same subset of ZMs can be used for the new rice sorting process.

Table 3 Performance of MLP classifier using the full and subset Zernike moment features

No. of hidden nodes	Accuracy (%)		Time saved (%)
	Full set	Subset	
5	93.0	98.0	66.91
10	94.0	98.0	66.34
15	95.0	98.0	69.72
20	96.0	98.0	66.54
25	96.0	98.0	67.04
30	96.0	98.0	68.75
Average	95.0	98.0	67.55

Also included the processing time saved when using full set and subset Zernike moments for rice sorting application

7 Conclusion

A novel rice sorting process is proposed in this paper to overcome the problems faced by the conventional rice sorting machine in terms of computational speed and sorting ability. ZMs with its rotational invariance property is selected to counter the orientation problem associated with the falling rice. Twelve orders of ZMs are utilized in this project. However, computing 12 orders takes a considerable amount of time, hence a subset of ZMs is used instead. The subset of ZMs is determined using the combination of FA and GA. To further reduce the computation time, the combination of q-recursive and the symmetry property of ZMs is utilized. The experimental results showed that the subset of ZMs takes one-third the processing time as compared with using the full set of ZMs while maintaining the classification accuracy. The mechanism of selecting a subset of ZMs shown in this paper can be applied for any classification application that uses ZMs as pattern features.

Acknowledgment The authors would like to extend their thanks to anonymous reviewers for the valuable and constructive comments for making this manuscript more readable.

References

1. Belkasim, S.O, Ahmadi, M., Shridhar, M.: Efficient algorithm for fast computation of zernike moments. In: Proceedings of IEEE 39th Midwest Symposium on Circuit and Systems, vol. 3, pp. 1401–1404 (1997)
2. Carpenter, G.A.: Distributed learning, recognition, and prediction by art and artmap neural networks. Neural Netw. **10**(2), 1473–1494 (1997)
3. Carpenter, G.A., Grossberg, S., Markuzon, N., Reynolds, J.H., Rosen, D.B.: Fuzzy artmap: a neural network architecture for incremental supervised learning of analog multidimentional maps. IEEE Trans. Neural Netw. **3**(5), 698–713 (1992)
4. Carpenter, G.A., Grossberg, S., Reynolds, J.H.: A fuzzy artmap nonparametric probability estimator for nonstationary pattern recognition problems. IEEE Trans. Neural Netw. **6**(6), 1330–1336 (1995)
5. Chong, C.W. Mukundan, R., Raveendran, P.: An efficient algorithm for fast computation of zernike moments. In: Proceedings of International Conference on Computer Vision, Pattern Recognition and Image Processing, pp 785–788, Durham, North Carolina (2002)
6. Chong, C.W., Raveendran, P., Mukundan, R.: A comparative analysis of algorithm for fast computation of zernike moments. Pattern Recognit. **36**(3), 731–742 (2003)
7. Chong, C.-W.: A Formulation of A New Class of Continuous Orthogonal Moment Invariants, and the Analysis of Their Computational Aspects. Dissertation, Faculty of Engineering, University of Malaya, 50603 Kuala Lumpur, Malaysia (2003)
8. Chong, C.W., Raveendran, P., Mukundan, R.: Translation invariants of zernike moments. Pattern Recognit. **36**(8), 1765–1773 (2003)
9. Gen, M., Cheng, R.: Genetics algorithms & engineering optimization. Wiley, New York (2000)
10. Ghosal, S., Mehrotra, R.: Edge detection using orthogonal moment-based operators. In: Proceedings of 11th Image, Speech and Signal Analysis (IAPR) International Conference on Pattern Recognition, vol. III, pp. 413–416 (1992)
11. Ghosal, S., Mehrotra, R.: Segmentation of range images: an orthogonal moment-based integrated approach. IEEE Trans. Robotics Autom. **9**(4), 385–39 (1993)
12. Goldberg, D.E.: Genetic algorithms in search, optimization and machine learning. Addison-Wesley, Reading (1989)
13. Haupt, R.L., Haupt, S.E.: Practical genetic algorithms. Wiley, New York (1998)
14. Holland, J.H.: Adaptation in natural and artificial systems. University of Michigan Press, Ann Arbor (1975)
15. Iskander, D.R., Morelande, M.R. Collins, M.J., Davis, B.: Modelling of corneal surfaces with radial polynomials. IEEE Trans. Biomed. Eng. **49**(4), 320–328 (2002)
16. Khotanzad, A.: Rotation invariant pattern recognition using zernike moments. In: Proceedings of International Conference on Pattern Recognition, pp. 326–328 (1988)
17. Khotanzad, A., Lu, J.H.: Classification of invariant image representations using a neural network. IEEE Trans. Acoust. Speech Signal Process. **38**, 1028–1038 (1990)
18. Khotanzand, A., Hong, Y.H.: Invariant image recognition by zernike moments. IEEE Trans. Patt. Anal. Mach. Intell. **12**(5), 489–497 (1990)
19. Kintner, E.C.: On the mathematical properties of the zernike polynomials. Opt. Acta **23**(8):679–680 (1976)
20. Liao, S.X., Pawlak, M.: On image analysis by moments. IEEE Trans. Patt. Anal. Mach. Intell. **18**(3), 254–266 (1996)
21. Liao, S.X., Pawlak, M.: On the accuracy of zernike moments for image analysis. IEEE Trans. Pattern Anal. Mach. Intell. **20**(12), 1358–1364 (1998)
22. Mukundan, R., Ramakrishnan, K.R.: Moment functions in image analysis. World Scientific Publishing, Singapore (1998)
23. Prata, Jr A., Rusch, W.V.T.: Algorithm for computation of zernike polynomials expansion coefficients. Appl. Opt. **28**(4), 749–754 (1989)
24. Pawlak, M.: On the reconstruction aspect of moment descriptors. IEEE Trans. Inf. Theory **38**(6), 1698–1708 (1992)
25. Teague, M.R.: Image analysis via the general theory of moments. J. Opt. Soc. Am. **70**, 920–930 (1980)
26. Teh, C.H., Chin, R.T.: On image analysis by the methods of moments. IEEE Trans. Pattern Anal. Mach. Intell. **10**(4), 496–512 (1988)
27. van Rooij, A.J.F., Jain, L.J., Johnson, R.P.: Neural Network Training Using Genetic Algorithms, Machine Perception Artificial Intelligence, vol. 26. World Scientific, Singapore (1996)
28. Wee, C.Y., Raveendran, P., Takeda, F.: New computation methods for full and subset zernike moments. Inf. Sci. **159**(3–4), 203–220 (2004)
29. Wee, C.Y. Raveendran, P. Takeda, F. Tsuzuki, T. Kadota, H., Shimanouchi, S.: Classification of rice grain using new scale invariant zernike moments. In: Proceedings of International Conference on Computer Vision, Pattern Recognition and Image Processing (CVPRIP'2002). Durham, South Carolina, USA (2002), pp. 832–835
30. Wee, C.Y., Raveendran, P. Takeda, F. Tsuzuki, T. Kadota, H., Shimanouchi, S.: Feature reduction of zernike moments using genetic algorithm for neural network classification of rice grain. In: Proceedings of International Joint Conference on Neural Networks (IJCNN 2002), vol. 1, pp. 1013–1018, Hawaii, USA (2002)
31. Wee, C.Y., Paramesran, R.: Efficient computation of radial moment functions using symmetrical property. Pattern Recognit. 39(11):2036–2046 (2006)

32. Wee, C.-Y., Paramesran, R., Takeda F.: Fast computation of zernike moments for rice sorting system. In: Proceedings of 2007 IEEE International Conference on Image Processing (ICIP 2007), vol. 6, pp. 165–168, San Antonio, Texas, USA (2007)
33. Zernikem, F.: Beugungstheorie des schneidenverfahrens und seiner verbesserten form, der phasenkontrastmethode. Physical 7:689–701 (1934)

Author Biographies

Chong-Yaw Wee received his B.Eng., M.Eng.Sc. and Ph.D. degrees in electrical engineering from University of Malaya, Malaysia, in 2001, 2003 and 2007, respectively. He is currently a post-doctoral research fellow in Centre for Signal and Image Processing (CISIP), Department of Electrical Engineering at University of Malaya. His research interests lie in the field of image and signal analysis, statistical pattern recognition and evolutionary computation. His present work includes developing novel degraded image recognition system, image/video quality assessment system using the orthogonal moment functions and statistical pattern recognition concepts.

Raveendran Paramesran received his B.Sc. and M.Sc. degrees in electrical engineering from South Dakota State University, Brookings, and the Dr. Eng. degree from University of Tokushima, Japan, in 1984, 1985 and 1994, respectively. He is currently a Professor in the Department of Electrical Engineering at University of Malaya. His research interests include image and signal analysis, video coding and Brain–Computer-Interface (BCI) technology. He is a Senior Member of IEEE. He is also a reviewer for IEEE Transactions on Pattern Analysis and Machine Intelligence (PAMI), Systems, Man, And Cybernetics (SMC) Part B: Cybernetics, Image Processing and also several other international journals.

Fumiaki Takeda received his Ph.D degree from the University of Tokushima, Tokushima Japan in 1994. He is currently a Professor in the Department of Intelligent Mechanical Systems Engineering, Kochi University of Technology, Japan. His research interests include Communication/network engineering, System engineering, Control engineering, neural networks, GA, intelligent recognition and digital signal processor.